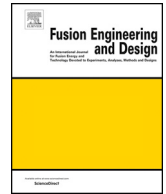




ELSEVIER

Contents lists available at ScienceDirect

Fusion Engineering and Design

journal homepage: www.elsevier.com/locate/fusengdes

The *dud* detector: An empirically-based real-time algorithm to save neutron and T budgets during JET DT operation

L. Piron^{a,b,c,*}, C. Challis^c, R. Felton^c, D. King^c, M. Lennholm^{d,e}, P. Lomas^c, C. Piron^b, F. Rimini^c, D. Valcarcel^c, JET Contributors¹

^a Dipartimento di Fisica "G. Galilei", Università di Padova, Padova, Italy

^b Consorzio RFX, Corso Stati Uniti 4, 35127, Padova, Italy

^c CCFE, Culham Science Centre, Abingdon, OX14 3DB, United Kingdom

^d European Commission, B-1049, Brussels, Belgium

^e EFDA Close Support Unit, Culham Science Centre, Abingdon, OX14 3DB, United Kingdom

ARTICLE INFO

Keywords:

JET
Plasma
Real-time control
DT

ABSTRACT

Operations using deuterium-tritium (DT) mixtures are envisaged in JET device in the forthcoming 2020 experimental campaign. These experiments will offer a unique possibility to study several open issues in support to ITER and DEMO, such as alpha particle heating, and to improve the high plasma performance obtained in the previous DT campaign Keilhacker et al. [1]. During DT operation, each plasma discharge will be a precious resource, being both T and neutron budget limited. It will be thus mandatory to promptly detect and safely terminate those plasma discharges which do not achieve the expected target parameters. A real-time detector of underperforming discharges has been developed for this purpose and it is named the *dud* detector. The *dud* detector calculates and monitors the time evolution of plasma performance indicators, which can be used to trigger an alarm and a proper plasma termination. The experience gained on the algorithm's behavior during DD operation will allow the use of this tool during DT operations and can be used as a guide to design *dud* detectors for ITER and future fusion reactors.

1. Introduction

The ultimate aim of fusion research is the production of fusion power. Substantial fusion power was produced in two large fusion devices: TFTR (10.7 MW) [2] and JET (16 MW) during its first Deuterium-Tritium (DT) campaign, DTE1 [1]. Such records were achieved by using equal concentrations of D and T since in this case the fusion reactivity is much higher than using other fuel mixtures, and thus more fusion reactions can occur.

In DT operations, care has to be taken to reduce the T inventory as much as possible to minimize any escape of T [3] and to restrict the total number of DT neutrons in order to limit the activation of the machine. The technological development for safe handling of T and for remote handling of activated materials is therefore required for such operation, and plasma experiments should be carefully scheduled to optimize the consumption of the limited T and neutron budgets, while maximizing the physics and engineering outcomes.

In the JET device, DT plasma operations are envisaged in the

forthcoming 2020 experimental campaign. JET, thanks to its capability to operate in T and the wide coverage of diagnostics, offers a unique and invaluable opportunity for testing new control algorithms for burning plasmas, to further progress our understanding in fusion power production and to extrapolate it towards ITER and the next step fusion reactors.

The upcoming JET DT campaign will be performed after major upgrades which have been carried out in the two decades since DTE1. Among the various upgrades, the most notable is the installation of a new Tungsten (W) and Beryllium first wall, i.e. the ITER-like wall (ILW), which replaces the previous Carbon (C) wall [4] and the availability of higher auxiliary heating power, in both the NBI and ICRH systems (~22.5 MW of NBI + ~3 MW of ICRH were available in DTE1, while ~34 MW of NBI + ~8 MW of the ICRH will be available in the forthcoming DT campaign). During the DT campaign, the plasma dynamics will be studied in various plasma scenarios which have been carefully optimized in the last decades to maximize the fusion performance.

* Corresponding author at: Dipartimento di Fisica "G. Galilei", Università di Padova, Padova, Italy.

E-mail address: lidia.piron@unipd.it (L. Piron).

¹ See the author list of "X. Litaudon et al 2017 Nucl. Fusion 57 102001.

<https://doi.org/10.1016/j.fusengdes.2019.02.077>

Received 8 October 2018; Received in revised form 24 January 2019; Accepted 18 February 2019

0920-3796/© 2019 Elsevier B.V. All rights reserved.

The 14 MeV DT neutron budget has been increased from 0.3×10^{21} in DTE1 to 2.1×10^{21} . The usage of T in any one day has been increased from ~ 2.4 barl to ~ 44 barl, thanks to the overnight regenerations of divertor and neutral beam cryogenic pumps [5]. T inventory and neutron activation will be monitored pulse by pulse, to rigorously fulfil the key safety requirements and the safety metrics adopted for DT operation.

To save neutron and T budgets during DT operation, it is highly desirable to use a real-time algorithm that safely stops underperforming plasmas, i.e. beta too low, fusion power below expectation, plasma not steady, or unhealthy conditions that will compromise the experiment goals, i.e. inadequate heating power, deleterious MHD activity, excessive radiation, incorrect fuel mixture.

One such *dud* detector algorithm has been developed, calculating and monitoring the time evolution of various plasma performance indicators, which can be used to trigger an alarm and a proper plasma termination.

In this work, Section 2 deals with the plasma performance indicators used in the *dud* detector for baseline and hybrid plasmas. Section 3 is focused on the reliability of the *dud* detector in identifying underperforming plasmas. Section 4 describes the integration of the *dud* detector with other real-time controllers which will be used in the forthcoming DT campaign and its coupling with a proper plasma termination. Section 5 gives the conclusions.

2. Development of the *dud* detector

In DTE1, a simple *dud* detector was used consisting in monitoring whether the neutron rate, R_{nt} , remained above a pre-determined curve [6]. This curve discriminated between plasmas showing ‘good’ and ‘bad’ performance.

Fig. 1(a–b) show the time behavior of the prescribed curve of the neutron rate, represented with a solid line, together with the measured R_{nt} and the NBI power of a ‘good’ and a ‘bad’ plasma performed during DTE1 [1], indicated with dashed and dotted lines, respectively. In the ‘good’ performing plasma, a peak of fusion power of about 12 MW was reached, before the high performance phase was terminated by a giant ELM, at around $t = 13.4$ s. This was the typical behavior of the so-called hot-ion H-mode, where the high performance phase was always terminated by a giant ELM after 1–2 s. In contrast, the aim of the upcoming DT campaign is to run stationary plasmas, maintaining reasonably

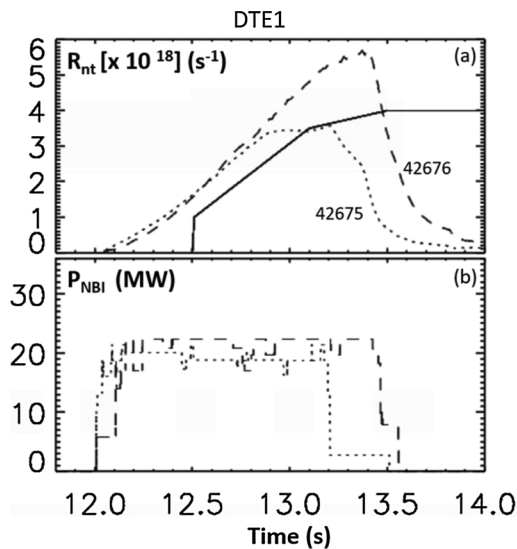


Fig. 1. Time behavior of (a) neutron rate and (b) NBI power of a ‘good’ and a ‘bad’ performing plasma during DTE1, represented with dashed and dotted lines, respectively. The solid line in panel (a) represents the pre-determined curve used to discriminate ‘good’ and ‘bad’ performance during DTE1.

steady fusion power for durations up to 5 s.

In preparation for DT experiments, a new *dud* detector has been developed. Underperforming plasmas can be identified by the *dud* detector on the basis of plasma performance indicators. If the plasma performance is not as expected, the *dud* detector can raise an alarm and initiate a plasma termination.

At present, the most promising indicators for *dud* detection are the $H_{IPB98(y;2)}$ and the neutron rate normalized to the plasma stored energy squared, R_{nt} / W_p^2 .

$H_{IPB98(y;2)}$ is the ratio between the plasma energy confinement time, τ_E , and the confinement time expected from the empirical, multi-machine energy confinement scaling law, $\tau_{IPB(y;s)}$, defined in [7]. In particular, τ_E , $\tau_{IPB(y;s)}$, and $H_{IPB98(y;2)}$ are expressed as follow:

$$\tau_E = W_{th}/P \quad (1)$$

$$\tau_{IPB98(y;s)} = 0.0562 I_p^{0.93} B^{0.15} n^{0.41} P^{-0.69} R^{1.39} k^{0.78} a^{0.58} M^{0.19} \quad (2)$$

$$H_{IPB98(y;s)} = \tau_E / \tau_{IPB98(y;s)} \quad (3)$$

where W_{th} is the plasma diamagnetic energy neglecting the energy associated with the fast ion energy [8], P is the loss power flowing across the separatrix, I_p is the plasma current, B is the magnetic field in vacuum, n the volume averaged density, R is the major radius, k is the plasma elongation, a is the minor radius and M is the main ion mass number.

The scaling of R_{nt} versus W_p^2 covers the dependence of the neutron rate from thermonuclear, beam-beam and beam-plasma reactions on the squared of thermal and fast particle energies. For a given species mixture, variations in the reactivity can arise from variations in plasma profiles, ion and electron temperature, impurity concentration and beam energy. Therefore any reduction with respect to the expected R_{nt}/W_p^2 scaling is considered as a symptom that the plasma is in distress.

$H_{IPB98(y;2)}$ and R_{nt}/W_p^2 are envisaged as plasma performance indicators since they are easily and robustly estimated on the basis of the available real-time signals on JET.

A statistical analysis of the plasma performance indicators has been carried out for a database of DD plasma discharges from 2015 to 2017 to empirically identify the thresholds that discriminate a ‘good’ and ‘bad’ plasma, and assess their dependence on the plasma scenario.

Fig. 2(a–b) show the time evolution of $H_{IPB98(y;2)}$ with respect to the switching on of the NBI system while Fig. 2(c–d) show R_{nt} as a function of W_p^2 . Each data point represents the mean value of the above mentioned quantities over 0.2 s, which is about an energy confinement time, to discard transients in the plasma behavior. Data has been calculated during the NBI heating phase since the NBI system is used in most JET discharges and since it provides more auxiliary heating power than the ICRH system. Data refers to baseline and hybrid scenarios, operational regimes that are investigated in JET machine in preparation to ITER operation [9].

Note that the statistical analysis shows that both the scenarios have reached $H_{IPB98(y;2)} > 1$, thus good energy confinement time, well above the empirical, multi-machine energy confinement scaling law. Moreover, the analysis demonstrates that the scaling factor from W_p^2 to R_{nt} depends on the plasma scenario. In fact each scenario follows different routes to achieve high neutron rate, thus high fusion power. The baseline scenario achieves high neutron rate by reaching the highest plasma stored energy, by operating at high plasma current, (up to 3.5 MA at present – higher in the future). Conversely, the hybrid scenario produces most neutrons per MJ of plasma stored energy, by operating in low density, high temperature plasma regimes.

Since the aim of the *dud* detector is to monitor the plasma performance, thresholds on the plasma performance indicators have to be defined for alarm generation. The thresholds on plasma performance indicators can be empirically identified considering the analyses reported in Fig. 2. It is worthwhile to stress that the thresholds valid for DD plasmas cannot be used directly for DT operation. For example, the

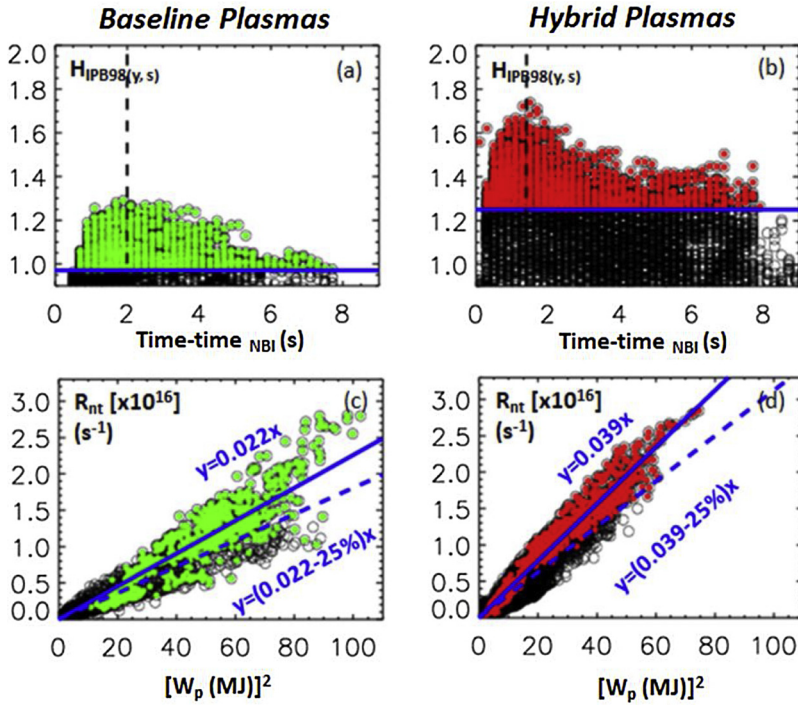


Fig. 2. (a–b) Time behavior of $H_{IPB98(y;2)}$ relative to the switching on of the NBI system and (c–d) neutron rate as a function of the plasma stored energy squared. Data with $H_{IPB98(y;2)} > 75\%$ of the maximum achieved $H_{IPB98(y;2)}$ is indicated in green and red for baseline and hybrid scenario, respectively. (For interpretation of the references to colour in this figure legend, the reader is referred to the web version of this article).

expression for $H_{IPB98(y;2)}$ depends on the ion mass number, thus on the fuel mixture. The latter also affects the neutron rate, which can be estimated using TRANSP [10] and JESTOOR [11] predictive modelling, for a given plasma scenario. This model-based prediction can provide a first indication of the threshold for *dud* detection, which will be optimized empirically as the DT plasma performance evolves.

For DT operation, the *dud* detector using $H_{IPB98(y;2)}$ and R_{nt}/W_p^2 as plasma performance indicators could be supplemented with other ITER-relevant metrics such as Q , the ratio between the fusion power and the power required to maintain the plasma in steady-state, and the normalized fusion gain G . G is defined as $G = \beta_N H_{IPB98(y;2)} / q_{95}^2$, where $\beta_N = \beta a / I_p$ and β is the plasma pressure normalized to the magnetic field pressure and q_{95} is the safety factor at 95% of the normalized poloidal flux [12].

3. Performance analysis of the *dud* detector

The algorithm behavior has been investigated, by running it offline, to choose the optimal options for the real-time implementation in order to strike the best compromise between false and missed detections. For this analysis, thresholds on the plasma indicators have been chosen and the plasma performance has been scrutinized in two time windows.

The criteria chosen to define a well performing or non-*dud* plasma are: $H_{IPB98(y;2)} > 75\%$ of the maximum $H_{IPB98(y;2)}$ achieved and the R_{nt}/W_p^2 ratio being more than the 75% of an empirical threshold defined in the following.

A threshold value equal to 75% of the maximum $H_{IPB98(y;2)}$ achieved has been chosen since it seems reasonable to consider plasmas which have high energy confinement time. The ensemble of data that fulfills this criterion is represented with full dots in Fig. 2, in green and red for baseline and hybrid plasmas, respectively.

Note that both the ensembles have energy confinement similar to, or greater than, the one statistically foreseen in other magnetic fusion devices, based on the trend reported in Eq. (2).

A plasma, besides having satisfactory energy confinement time, should also have large reactivity. The empirically defined threshold of R_{nt}/W_p^2 has been determined by using a linear regression method on the ensemble of data that has $H_{IPB98(y;2)} > 75\%$ of the maximum

achieved $H_{IPB98(y;2)}$. The result of the linear regression is indicated with a solid line in Fig. 2(c–d). In the same figures, the lower threshold value, i.e. 75% of the empirically identified one, is shown as a dashed line. Note that the R_{nt}/W_p^2 threshold of the baseline scenario differs from the one for hybrid scenario because these scenarios reach high neutron rate through different routes, as discussed in the previous section.

The plasma performance has been classified based on 5 possible types of behavior, reported in Table 1. These types of behavior, representing the different plasma performance trajectories that can occur, have been scrutinized on two time windows, $\Delta T1$ and $\Delta T2$, as represented in the sketch reported in Fig. 3.

The algorithm has been set up to avoid premature *dud* detection. As a matter of fact, the detector exploited during DTE1 was not activated from the beginning of the NBI phase, but 0.5 s after it is switched on, as shown in Fig. 1(a), to allow the plasma to enter in H mode and to improve its performance. Similarly, in the new version of the *dud* detector, a warming-up time has been introduced. The warming-up time has been empirically tuned to minimize the premature *dud* detection and it is about 1 s for the baseline scenario and 0.4 s for the hybrid scenario.

The *dud* detector does not raise an alarm during the warming-up phase. However, if in this phase the auxiliary heating power will be inadequate and/or the impurity content will be unacceptable for the target experiment, the *dud* detector can still terminate the discharge early.

Table 1

Statistics of plasma performance in baseline and hybrid plasmas considering the plasma performance criteria and during the time intervals described in the text. The numbers which are not in brackets refers to a length of window $\Delta T2$ of 0.5 s, while the numbers in brackets refers a length of window $\Delta T2$ of 1.0 s.

$\Delta T1$	$\Delta T2$	Baseline (%)	Hybrid (%)
Non- <i>dud</i>	Non- <i>dud</i>	52 (45)	42 (34)
Non- <i>dud</i>	<i>Dud</i>	11 (17)	6 (14)
<i>Dud</i>	<i>Dud</i>	29 (31)	41 (43)
<i>Dud</i>	Non- <i>dud</i>	5 (4)	9 (7)
<i>Dud</i> / Non- <i>dud</i>	No samples	3 (3)	2 (2)

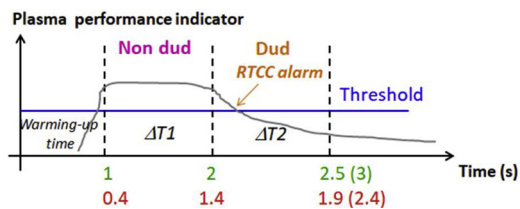


Fig. 3. Sketch representing *dud* detection based on a possible time evolution of a plasma performance indicator in a baseline or hybrid plasma and the corresponding threshold value which discriminates a plasma with ‘good’ (non-*dud*) and ‘bad’ (*dud*) performance.

The statistical analyses of $H_{IPB98(y;2)}$ versus time reported in Fig. 2(a–b) suggest a possible timing for detecting *dud* plasmas. Baseline plasmas reach the best plasma energy confinement after about 2 s of the switching on of the NBI power, while the maximum performance in hybrid plasmas is reached after 1.4 s. As represented in the sketch reported in Fig. 3, $\Delta T1$, the first time window for plasma performance investigation, has been then chosen to last from 1 s to 2 s for baseline plasmas, from 0.4 s to 1.4 s for hybrid plasmas. Two different durations of the second time window $\Delta T2$, i.e. 0.5 s and 1 s, have been chosen arbitrarily to study how the plasma performance evolves with time.

The performance analysis of the *dud* detector algorithm during $\Delta T1$ and $\Delta T2$ is summarized in Table 1. Notably, the numbers which are not in brackets refers to a length of window $\Delta T2$ of 0.5 s, while the numbers in brackets refers a length of window $\Delta T2$ of 1.0 s. This analysis shows that a large fraction of hybrid and baseline plasmas has good performance: more than 60% and almost 50% of baseline and hybrid plasmas, respectively, can be classified as non-*dud* in $\Delta T1$. Note that the number of false triggering alarms, i.e. plasmas that are seen as *duds* in $\Delta T1$ and non-*duds* in $\Delta T2$, is relatively small, proving that the algorithm is well tuned. The statistics of $\Delta T2$ with different time durations highlights that some discharges, despite having good performance in $\Delta T1$, are becoming *dud* plasmas in $\Delta T2$, for example, because of impurity accumulation and deleterious MHD activity. Various real-time controllers have been developed to avoid or to alleviate the effect of such events on the plasma dynamics [6] and these will be tested in the upcoming experimental campaign.

It is worthwhile stressing that the time windows shown in Fig. 3 have been defined only to perform the algorithm performance study. During plasma operation, the *dud* detector will monitor the plasma performance continuously, with alarms being issued as soon as the performance is deemed unsatisfactory. An assertion time over 0.2 s, which is about an energy confinement time, has been envisaged to allow the plasma to recover from transient events.

In the upcoming DD operation, the present version of the *dud* detector could be already exploited to build up experience in view of DT operation and, more specifically, to develop non-disruptive responses to a trigger, as discussed in the following section.

As mentioned in the previous section, TT operation is also planned in the JET device before DT experiments. During TT operation, the *dud* detector should be used to minimize consumption of T. In this case, the plasma performance indicator R_{nt}/W_p^2 will not be a metric of plasma performance but will represent the content of D in T plasmas. Therefore, new plasma performance indicators should be adopted for *dud* detection. The development of the *dud* detector and other real-time controllers for TT operation will be described in a dedicated paper.

4. Integration of the *dud* detector with other real-time algorithms and ad-hoc plasma termination

The *dud* detector during DT operation will work in synergy with other real-time algorithms. First of all, the isotope mixture control will be of fundamental importance to guarantee the optimal DT mixture (~50/50) to achieve maximum fusion power. This algorithm, which is

under-development and will be described in details in a separate paper, will allow the real-time control of multiple gas valve opening and beam waveforms. If the required DT fuel balance wouldn’t be obtained because of gas system failure, for example, the *dud* detector will trigger an alarm. Besides this, the *dud* detector will work in combination with other real-time algorithms available in the real-time central control system (RTCC) which allow for steady-state plasma operations by controlling a large number of plasma properties by using the additional heating and fueling systems as actuators. Examples of controlled parameters are plasma density, beta, ELM frequency and thermal load.

Once an alarm is triggered by the *dud* detector, the response is handled to by the JET real-time protection sequencer (RTPS). The nature of the response will depend on the plasma scenario and will trigger appropriate actions to terminate the plasma rapidly and safely, without inducing a disruption. During DT operation, it will be essential that the RTPS stops the T fueling as soon as possible, to minimize the T inventory, and decreases additional heating power to minimize the neutron production. The optimal recipe for plasma landing will be identified in the upcoming experimental campaign where dedicated experimental time is allocated for testing a range of termination scenarios.

5. Conclusion

JET, uniquely among present-day fusion experiments, will offer the capability of operating in DT, making its results particular relevant for advancing the physics and operational knowledge needed for the realization of a fusion reactor.

In preparation for such operation, the development of a real-time algorithm that optimizes the consumption of T and neutron budgets has been developed and presented in this work. The *dud* detector relies on plasma performance indicators to judge the evolution of the discharge. If a pulse is deemed not to be performing sufficiently well, the *dud* detector will raise an alarm and instigate a proper plasma termination.

In the near future, the *dud* detector could also be coupled with the advanced real-time plasma state observer RAPTOR [13], which is under development in JET. This tool will allow the identification of optimal actuator trajectories to improve the plasma performance, supporting the plasma scenario development and providing plasma performance indicators for *dud* detection. Furthermore, RAPTOR can detect and handle diagnostic faults by providing model-based estimation of plasma signals, thus improving the reliability of real-time control.

The experience gained on the *dud* detector’s behavior during JET DT operation can be used as a guide to design *dud* detectors for ITER and future fusion reactors, which will use the same DT fuel mixtures to achieve high fusion power.

Acknowledgments

This work has been carried out within the framework of the EUROfusion Consortium and has received funding from the Euratom research and training programme 2014-2018 under grant agreement No 633053. The views and opinions expressed herein do not necessarily reflect those of the European Commission. This project has also received funding from the RCUK Energy Programme [grant number EP/012450/1]. To obtain further information on the data and models underlying this paper please contact PublicationsManager@ccfe.ac.uk.

References

- [1] M. Keilhacker, et al., Nucl. Eng. 39 (209) (1999).
- [2] J.D. Strachan, et al., Phys. Rev. Lett. 22 (3526) (1994).
- [3] E.E. Belonohy, et al., Czech Republic, September 5–9 Technical Rehearsal of DT Operation at JET 29th Symposium on Fusion Technology (SOFT) Prague2016, Technical Rehearsal of DT Operation at JET 29th Symposium on Fusion Technology (SOFT) Prague (2016).
- [4] F. Romanelli, et al., Nucl. Eng. 53 (104002) (2013).

- [5] S. Carvalho Ivo, et al., Fusion Eng. Des. 124 (2017) 841–845.
- [6] M. Lennholm, et al., Fusion Eng. Des. 123 (2017) 535–540.
- [7] ITER physics basis expert groups on confinement and transport and confinement modelling and database, ITER physics basis editors, Nucl. Eng. 39 (1999) 2175–2249.
- [8] G. Fishpool, et al., Nucl. Eng. 38 (1372) (1998).
- [9] I. Nunes, et al., Plasma Phys. Control. Fusion 58 (2016) 014034.
- [10] <http://w3.pppl.gov/share/help/transp.htm>.
- [11] C.D. Challis, private communication (2018).
- [12] A.C. Sips, et al., Phys. Plasmas 22 (2015) 021804.
- [13] F. Felici, et al., Plasma Phys. Control. Fusion 54 (2012) 024002.